



ELSEVIER

Journal of Crystal Growth 232 (2001) 399–408

JOURNAL OF
**CRYSTAL
GROWTH**

www.elsevier.com/locate/jcrysgro

Crystallogenesi s in tRNA aminoacylation systems: how packing accounts for crystallization drawbacks with yeast aspartyl-tRNA synthetase

C. Sauter¹, B. Lorber, A. Théobald-Dietrich, R. Giegé*

Département Mécanismes et Macromolécules de la Synthèse Protéique et Cristallogénèse, UPR 9002, Institut de Biologie Moléculaire et Cellulaire du CNRS, 15 rue René Descartes, 67084 Strasbourg Cedex, France

Abstract

Two active forms of homodimeric aspartyl-tRNA synthetase from *Saccharomyces cerevisiae* differing in length at their N-terminus crystallize in the same orthorhombic space group ($P4_12_12$) with identical cell parameters. Initial studies were hampered by the poor and anisotropic diffraction of the crystals of enzyme extracted from yeast cells. Isotropic diffraction at higher resolution was obtained when crystals were grown from an engineered protein deprived of its 70 N-terminal amino acids. The present work describes the packing contacts in crystals of the shortened protein whose structure was solved at 2.3 Å resolution. Each subunit of the enzyme develops two lattice interactions covering a surface of 670 Å², about 7-fold smaller than that of the interface between monomers. The smallest lattice interaction, covering 150 Å², brings the anticodon binding domain adjacent to the N-terminus of one monomer in contact with a loop from the active-site domain of a neighboring monomer. Modeling of the extension in the solvent channels shows that the 150 Å² intermolecular contact is perturbed in protein molecules possessing a floppy appendix while their second and larger 520 Å² contact area is unaffected. Altogether the packing organization explains the poor diffraction properties of the native enzyme crystals and the enhanced diffraction of the crystals of shortened synthetase. © 2001 Elsevier Science B.V. All rights reserved.

PACS: 61.10.N; 61.72; 81.10.Dn; 87.15; 87.15.Kg

Keywords: A1. Crystal packing; A1. Crystal structure; A1. X-ray diffraction; A2. Growth from solutions; B1. Aspartyl-tRNA synthetase; B1. Proteins

1. Introduction

The biological importance of tRNAs and aminoacyl-tRNA synthetases attracted soon the

interest of biologists. However, great difficulties encountered in the course of their crystallization hampered the rapid development of structural biology in the field of genetic information translation. Nevertheless, researchers effort to understand and improve the crystallization of tRNAs, aminoacyl-tRNA synthetases, and complexes between both of them (reviewed in [1,2]) gradually contributed to the emergence of a field dedicated to macromolecular crystallogenesi s. These efforts led

*Corresponding author. Tel.: +33-3-88-41-70-58; fax: +33-3-88-60-22-18.

E-mail addresses: r.giege@ibmc.u-strasbg.fr (R. Giegé).

¹Present address: EMBL Heidelberg, Meyerhofstrasse 1, 69012 Heidelberg, Germany.

in particular to the development of novel crystallization techniques, like the vapor diffusion method first employed for tRNA crystallization [3] and the statistical methods using incomplete factorial experiments initially designed for an aminoacyl-tRNA synthetase crystallization [4]. Likewise, a number of characteristic features in crystal growth of small molecules were found in the macromolecular world when studying tRNAs and synthetases. Along these lines was the perception of the key role of purity in macromolecular crystallization [5]. Thus, samples have to be pure not only in terms of lack of contaminants but also in terms of chemical and conformational homogeneity. This concept was verified using light scattering techniques in the case of synthetases that need to be homogeneous and monodispersed to nucleate [6,7]. Later, the study of the crystal growth of a tRNA by atomic force microscopy allowed to visualize the different types of growth mechanisms known for small molecules and proteins, and to show the great sensitivity of the crystal growth of this RNA to supersaturation variations [8]. A phase diagram study led to a similar conclusion in the case of a synthetase [9]. From another point of view, the discovery that ammonium sulfate at high concentration does not disrupt protein/RNA complexes was of crucial importance in crystallizing the complex between yeast tRNA^{Asp} and its cognate aspartyl-tRNA synthetase (AspRS) [10,11]. Later on, this was generalized to a great number of other nucleoprotein complexes [2]. Finally, analysis of the packing of yeast tRNA^{Asp} crystals allowed to understand why tRNA samples that were partially degraded in the anticodon loop did not crystallize and gave biological meaning to packing induced conformational changes in the tRNA molecule [12–14].

Here, we review briefly the 20 year story of yeast AspRS crystallization. We show how the knowledge of the recently solved structure [15] can help to understand a number of experimental difficulties which were encountered while attempting to improve the quality of AspRS crystals. In particular we discuss the importance of proper structure engineering for optimal crystallizability and recall how phase diagram data can be used to find better crystallization conditions. We give special

emphasis to the analysis of the packing contacts in yeast AspRS crystals and to how they account for differences in the properties of crystals grown from native enzyme and a truncated form.

2. Materials and methods

2.1. Materials, protein crystallization methods, and crystallographic analysis

Native AspRS from yeast is a homodimeric protein of Mr 128,000 with subunits of 557 amino acids each [16] with a monomer of modular structure (Fig. 1a).

In the first stages of this work, AspRS was isolated from commercial baker's yeast cells harvested in their exponential growing phase. Purification was done as described under conditions minimizing proteolytic degradation [17]. Batch dependent heterogeneity was revealed by electrophoresis and isoelectric focusing (Fig. 1b). The enzyme form used to solve the structure of the synthetase was truncated by 70 residues in its N-terminus (AspRS-70) and purified from over-producing *Escherichia coli* cells as described [9]. Its heterogeneity is negligible (Fig. 1b).

Crystals of AspRS-70 were grown by vapor diffusion in sitting drops using ammonium sulfate as the crystallizing agent [9]. Two crystal forms were obtained, either tetragonal (P4₁2₁2) or trigonal (P3₂21), both diffracting X-rays at a resolution better than 3.0 Å (the second with a pronounced anisotropy). Their solvent content was determined as described by Matthews [18]. Crystals were analyzed under cryogenic conditions using synchrotron radiation and diffraction limits in Table 2 indicate the highest resolution at which reflections with significant intensities ($I/\sigma(I) > 3$) were observed (see also diffraction patterns in Fig. 2). Thus, complete data were measured for a trigonal crystal (completeness of 86% between 3 and 28 Å, but anisotropic data) on the synchrotron beamline DW32 ($\lambda = 0.96$ Å, MarResearch IP 345 detector) at LURE [9]. Further, a 2.3 Å resolution data set (completeness of 98% between 2.3 and 20 Å, isotropic data) was collected for the tetragonal form on the ID14/EH4 beamline at ESRF

($\lambda = 0.94 \text{ \AA}$, Quantum CCD detector) [15]. The tetragonal structure was solved by molecular replacement using latter high resolution data and the coordinates of the yeast AspRS in the complex with the tRNA. The model was refined to a resolution of 2.3 \AA with a crystallographic R -factor of 20.2% and a R_{free} -factor of 24.2% [15].

2.2. Methods for crystal packing analysis

Intermolecular contacts in the tetragonal crystal lattice were examined with programs from the *CCP4 suite* [19]. *CONTACT* was used to determine the proximity between symmetry related molecules. Residues are admitted to be in contact when their atoms were separated by less than 3.6 \AA . Areas of buried surfaces were calculated using *AREAIMOL*. Accessible surfaces were computed with a probe of 1.4 \AA according to [20]. Packing pictures were plotted with *SETOR* [21] and accessible surfaces with *WebLab Viewer Lite* (<http://www.mci.com>). The putative N-terminal region was modeled according to the 2D structure predictions. The C^{α} chain was built in the solvent channels in a manner that avoids sterical hindrance from symmetrical molecules using the program *O* [22].

3. Results and discussion

3.1. The aspartate system from yeast: two decades of crystallization efforts

Structural investigations on the yeast aspartylation system started at the end of the seventies and Table 1 summarizes the whole story. The goal was to solve the structure of both the tRNA and the synthetase in a free state and that of their complex. Crystals of tRNA^{Asp} were rapidly obtained [23] and led the second high resolution structure of such a molecule [24]. At the beginning of the eighties, first tetragonal crystals of the free synthetase were grown [25] but crystallizability of the protein and diffraction properties of AspRS crystals fluctuated. In the meantime, crystals of the complex were grown: the first ones were cubic and diffracted only at low resolution [10,11,26], but

Table 1

From the protein purification to its 3D structure: a summary of the yeast AspRS story

1973	First purification of yeast AspRS [38]
1976	Start of crystallization attempts on the yeast aspartate system
1977	First crystals of tRNA ^{Asp} [23]
1980	X-ray structure of tRNA ^{Asp} [24] First crystals of free AspRS [25] First crystals of AspRS/tRNA ^{Asp} complex [10]
1983	Large scale purification protocol and dimeric nature of AspRS [17] AspRS microheterogeneity revealed by isoelectric focusing [39]
1985	Characterization of the yeast AspRS gene [16]
1986	Importance of purity in crystallization, based on observations in the yeast aspartate system [5]
1987	Identification of sequence microheterogeneities in AspRS [29]
1988	Improved crystals of the complex [27]
1990	Design and cloning of deletants for crystallization purposes [40]
1991	X-ray structure of AspRS/tRNA ^{Asp} complex [28]
1994	Initiation of a crystallogenesis strategy for free AspRS
1999	Two free AspRS crystal forms diffracting at high resolution [9]
2000	X-ray structure of free AspRS [15]

later efforts put on the enzyme purification proved to be worthwhile and orthorhombic crystals diffracting at a 3.0 \AA resolution were finally obtained [27]. Soon after, the structure of the complex was solved [28].

3.2. Protein engineering to improve the crystallization of free AspRS

Throughout this period, attempts to reproduce and improve the crystals of the free enzyme were continued. A first explanation for their poor quality came from sequence analysis. Indeed, this poor crystallizability was correlated with a structural heterogeneity of the protein extracted from yeast cells, which was always a mixture of polypeptide chains starting somewhere between residues 14 and 33 (Fig. 1) [29,30]. Further biochemical experiments indicated that the 70 first residues are not required for catalytic activity [30,31] and crystallography showed that the

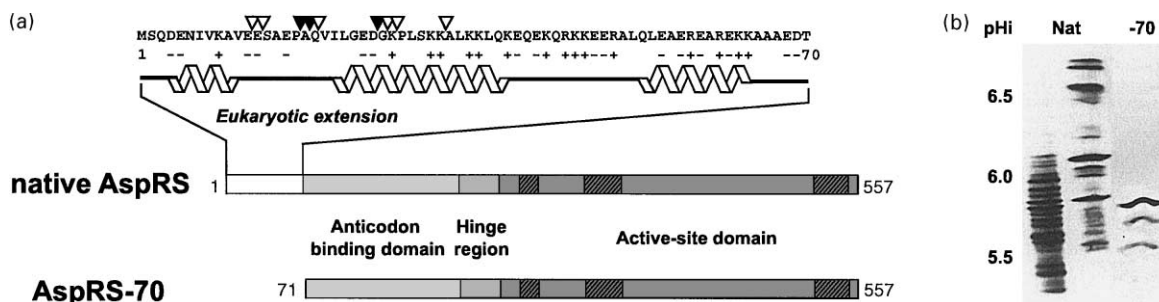


Fig. 1. Design of a truncated AspRS form. (a) Primary structure of yeast AspRS and its modular organization in the native enzyme purified from yeast and in the truncated AspRS-70 form. The AspRS monomer contains three structural domains: the anticodon binding domain in N-terminus, the connecting hinge region, and the active-site domain in C-terminus which carries three sequence consensus motifs (hashed boxes). In the AspRS purified from yeast (a-top), the N-terminal region is heterogeneous due to proteolysis: white and black arrows indicates minor and majors sites of proteolysis, according to [30]. This extension encompassing the 70 N-terminal residues is peculiar to eukaryotes and is not required for aminoacylation activity. Secondary structure prediction indicates that the extension is likely to form three α -helices [36]; a helical structure has actually been demonstrated for a synthetic 23-residue-long peptide derived from the extension [37]. This extension has been removed in the form called AspRS-70 (a-bottom). (b) Isoelectric focusing analysis under non-denaturing conditions. The experiments illustrate the heterogeneity differences between two different AspRS batches purified from yeast (on the left) and the dramatic increase in homogeneity in AspRS-70 (on the right).

heterogeneous N-terminal extension of the protein is disordered in the AspRS/tRNA^{Asp} complex [28,32].

On the basis of these biochemical and structural data, the idea of engineering a mutant of yeast AspRS lacking its first 70 N-terminal residues (AspRS-70) emerged. As anticipated, the biochemical characterization of this new AspRS form overexpressed in *E. coli* showed a dramatic improvement in homogeneity [9] as can be noticed by isoelectric focusing (Fig. 1b). This AspRS-70 active variant eventually led to high quality crystals.

3.3. Two crystal forms for free AspRS

Tetragonal and trigonal crystals were obtained as the result of a rational search of crystallization conditions at low protein supersaturation in a crystal-solution phase diagram [9]. Typical crystal habits and diffraction patterns are shown in Fig. 2 and crystallographic data are summarized in Table 2. Interestingly, tetragonal crystals have exactly the same bipyramidal morphology than those obtained in the early 80s with the larger and heterogeneous AspRS. In addition, they belong to the same space group and have identical cell

parameters, but the resolution limit is dramatically enhanced and extends isotropically to a resolution of 2.0 Å (Fig. 2a). In contrast, the trigonal prisms are clearly anisotropic and diffraction limit is highest in the direction corresponding to parameter *c* which is parallel to the crystallographic screw axis 3_2 (Fig. 2b). It is noticeable that under non-optimal conditions (lower pH, higher temperature or protein concentration), the habit of this form is needle-like (Fig. 2b), the crystals being elongated in the direction of higher diffraction, suggesting a better packing along the screw axis.

It is striking that highest diffraction quality (Table 2) is obtained with the crystal form having the lowest solvent content and, presumably, the highest density of crystal contact. This feature seems to be a general characteristic of aminoacyl-tRNA synthetase crystals [33].

Molecular replacement solutions were found in both tetragonal and trigonal space groups. Nevertheless, the quality of the electron density map calculated from trigonal data was low due to their characteristic anisotropy and the structure was finally solved at a nominal resolution of 2.3 Å (top of Fig. 3) using the tetragonal data [15].

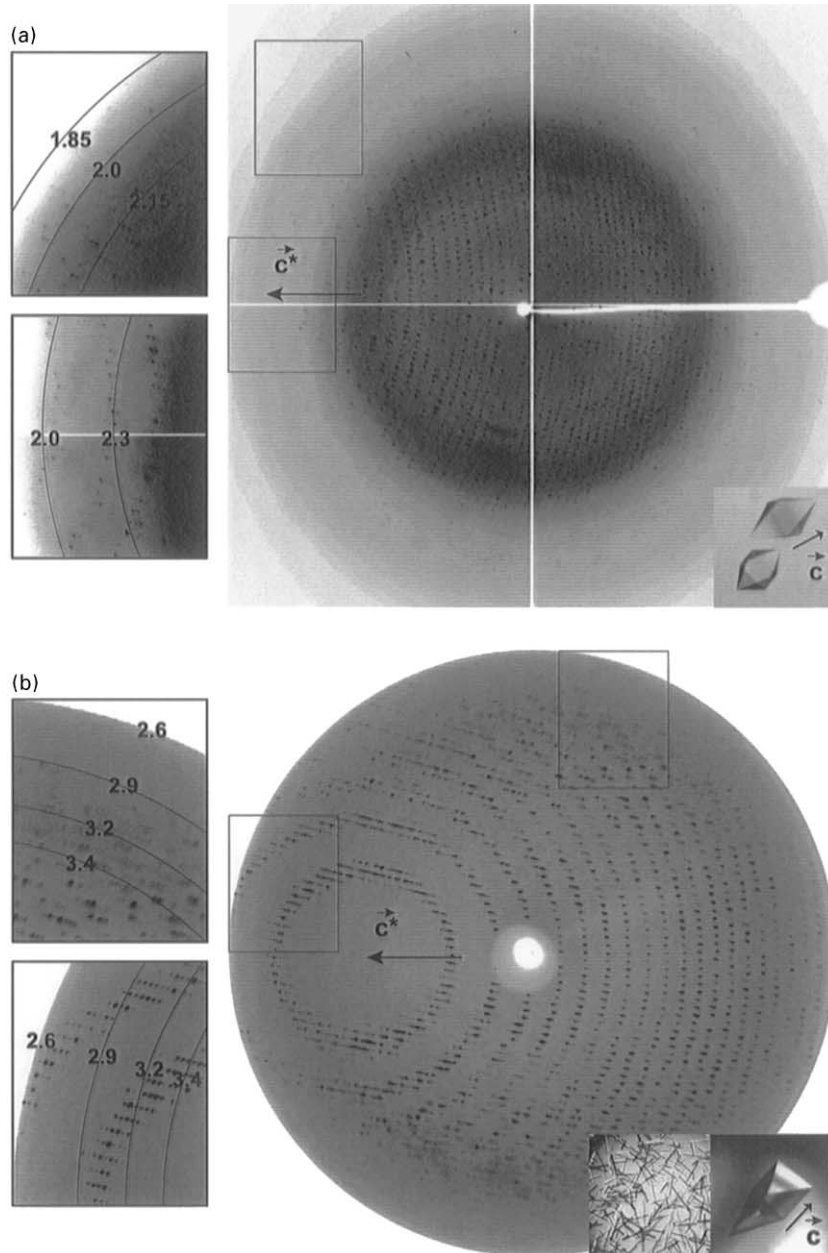


Fig. 2. Diffraction properties of yeast AspRS crystals. Windows on the left display close-up views of the diffraction patterns with the corresponding rings of resolution (in Å). Windows on the right hand side show the respective crystal habits: (a) tetragonal bipyramids and (b) trigonal thin needles or prisms. Diffraction patterns were collected with the crystals mounted in such a way that their c axis lies along the oscillation axis; the corresponding c^* axis (the shortest reciprocal cell parameter) is in the horizontal plane. (a) Oscillation image (0.5°) of a tetragonal crystal on the synchrotron beamline ID14/EH4, ESRF, Grenoble, France (Quantum CCD detector). The diffraction is isotropic up to 2.0 \AA of resolution. (b) Oscillation image (1°) of a trigonal crystal on the synchrotron beamline DW32, LURE, France (IP MarResearch 345 detector). This crystal form is characterized by an anisotropic diffraction: reflections can be measured at a resolution of 2.6 \AA and even higher in the c^* axis direction, whereas diffraction spots disappear beyond $3.4\text{--}3.5 \text{ \AA}$ in a perpendicular direction.

3.4. Tetragonal packing

The tetragonal crystal packing of dimeric AspRS-70 is illustrated in Fig. 3. The asymmetric unit contains one monomer, meaning that the dimer is fully symmetrical. The interface between monomers corresponds to an area of 4600 \AA^2 . Beside this natural contact, each monomer of the yeast enzyme develops two types of lattice interactions. They are shown in the top panel of Fig. 3, where contacts are emphasized in purple, and in the middle part of the figure, where the overall packing organization is displayed. Contact area A brings together two loops in the anticodon domain from the monomer (zone a with residues 119–121 and 219–222) and two loops from the catalytic domain of a neighbor molecule (zone a' with residues 410–417 and 495–500). In total, these contacts cover a surface of 520 \AA^2 . Surface of contact area B is more limited (150 \AA^2) and involves essentially a loop from the anticodon binding domain adjacent to the N-terminus (zone b with residues 145–147) and a loop from the active-site module of a neighboring monomer (zone b' with residues 390–395). The nature of

the contacts is summarized in Table 3. Altogether, 20 amino acids participate in 12 well defined amino acid ↔ amino acid interactions involving predominantly hydrogen-bonds and Van der Waals contacts, but no ionic interaction. This contrasts with what observed for AspRS-1 from *Thermus thermophilus* which mainly develops hydrophobic Van der Waals interactions in two different lattices [34]. In the yeast enzyme the contact amino acids form eight discrete interaction patches distributed between the anticodon binding domain and the catalytic domain (Fig. 3, top).

As described by Janin for dimeric proteins [35], we note in the case of AspRS a dramatic difference between the oligomerization contacts and the crystal lattice contacts, the dimer interface (4600 \AA^2) being about 7 times larger than the scattered packing surface (670 \AA^2).

3.5. The truncated protein favors one contact

As seen in Fig. 3, contact B takes place close to the N-terminus of AspRS-70 in a lattice region where room for intermolecular solvent is limited. Since tetragonal crystals, as obtained by Dietrich

Table 2
Characterization of AspRS crystal forms

Crystal form	Tetragonal (I)	Trigonal (II)
Crystal habit	Bipyramids	Prisms with triangular basis
Typical crystal size (mm^3)	$0.4 \times 0.4 \times 0.6$	$0.3 \times 0.3 \times 0.7$
Space group	$P4_12_12$	$P3_221$
Unit cell lengths (\AA)	$a = 90.2, c = 185$	$a = 111, c = 244$
Diffraction limit (\AA)	~ 2.0	~ 2.6 (anisotropic)
Asymmetric unit	1 monomer	1 dimer
Solvent content (%)	64	69
Matthews V_m coeff. ($\text{\AA}^3/\text{Da}$)	3.4	4.0

Fig. 3. Details of the packing in tetragonal AspRS-70 bipyramids. (Top) On the left, the AspRS-70 dimer is represented with its crystallographic 2-fold axis pointing toward the reader. Zones involved in packing contacts are colored in purple on the yellow monomer which correspond to the asymmetric unit content. Arrows indicate regions in zones a, a', b, b' which are involved in packing interactions. (Middle) The dimer surrounded by its closest neighbors (in blue) in the tetragonal unit cell. Arrows point the zones a and b of the yellow monomer which are involved in contacts A and B, respectively. The purple square indicates the region which is enlarged in the bottom panel. (Bottom) Close-up view of the packing in the N-terminal region of the AspRS monomer. The 70 N-terminal residues have been modeled in the solvent channel according to the secondary structure prediction. The segment in orange corresponds to the extension (45 residues) which was present on average in the native crystals. The white segment (25 residues) was absent due to proteolytic degradation but would be present in a full-length enzyme crystallizing in this lattice.

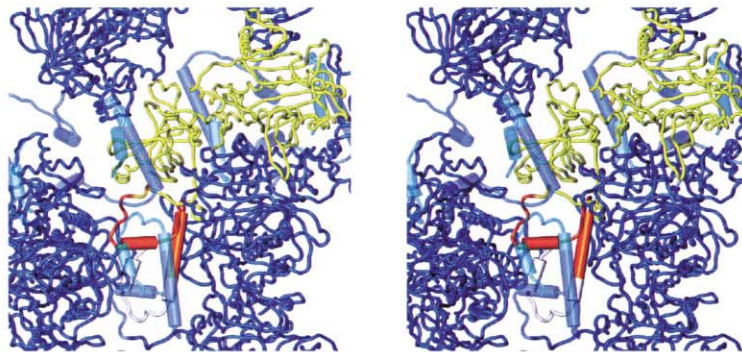
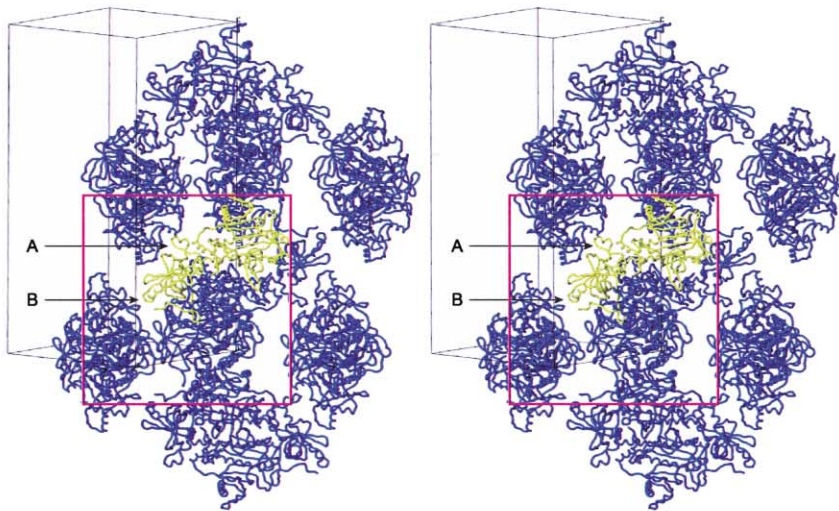
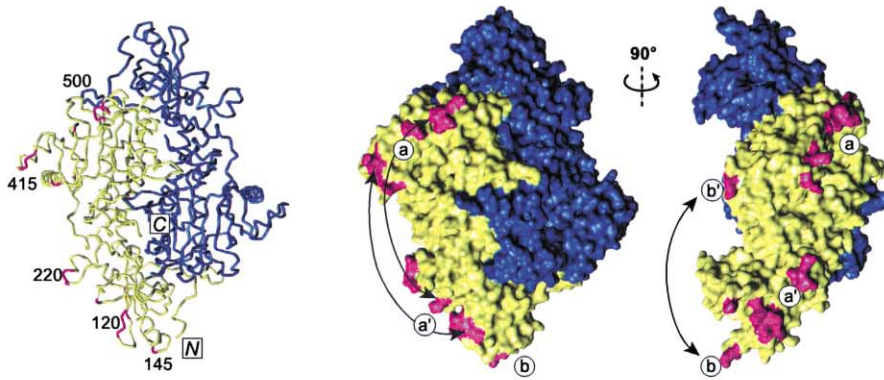


Table 3
Molecular contacts in the tetragonal packing

Contacts between monomers ^a		Residues in interaction ^b		Buried surface
A	zone a ↔ zone a'	<i>R</i> 119 ↔ <i>I</i> 416 ^h	<i>E</i> 219 ↔ <i>H</i> 499 ^h	520 Å ²
	$x, y, z \leftrightarrow 1/2 + x, 1/2 - y, 1/4 - z$	<i>Q</i> 121 ↔ <i>K</i> 414 ^h	<i>E</i> 219 ↔ <i>G</i> 500 ^{vw}	
	$1/2 + x, 1/2 - y, 1/4 - z \leftrightarrow x, y, z$	<i>F</i> 127 ↔ <i>E</i> 415 ^{vw}	<i>A</i> 220 ↔ <i>H</i> 499 ^h	
		<i>Q</i> 138 ↔ <i>E</i> 415 ^h	<i>A</i> 221 ↔ <i>E</i> 451 ^{vw}	
		<i>E</i> 177 ↔ <i>E</i> 425 ^h	<i>G</i> 222 ↔ <i>A</i> 498 ^h	
		<i>G</i> 222 ↔ <i>R</i> 495 ^h		
B	zone b ↔ zone b'	<i>K</i> 145 ↔ <i>K</i> 393 ^h		150 Å ²
	$x, y, z \leftrightarrow 1/2 + y, 1/2 - x, z - 1/4$			
	$x - 1/2, 1/2 - y, 3/4 - z \leftrightarrow x, y, z$			

^a Each monomer (x, y, z) develops 4 packing contacts which are either of type A or of type B. The corresponding interaction zones (a, a', b, b') are shown in Fig. 3 (top). The natural dimer interface involves monomers x, y, z and $-y, -x, 1/2 - z$ and corresponds to a buried surface area of 4600 Å².

^b Amino acid residues taking part to lattice interactions are indicated in one letter code. They develop hydrogen bonds (h) or Van der Waals (vw) interactions involving either their backbone atoms (residues in normal letter) or their side chain atoms (residues in italic).

et al. [25] with an AspRS longer by 45 residues on average than AspRS-70, belong to the same space group with identical parameters, we conclude that in the longer enzyme the additional N-terminal heterogeneous extension must be accommodated in the available solvent volume found in the AspRS-70 lattice. As a consequence, the bulkiness of the heterogeneous extension likely alters packing interaction B. Although the exact reason of this alteration is not known (poisoning of the crystal growth by some of the isoforms of the extension, or intrinsic property of the extended enzyme to disturb the packing), it contributes to the poor crystallizability of the enzyme extracted from wild-type yeast cells.

To test this interpretation we have modeled the N-terminal extension of AspRS in the tetragonal lattice of AspRS-70 crystals (Fig. 3, bottom). For that we have taken into account the fact that the 70 amino acid N-terminal extension is flexible in the absence of tRNA and most likely adopts a secondary structure made of three helices connected by loops (Fig. 1a). This assumption is based on structure prediction and on a thorough biochemical and mutagenesis analysis of the extension [36]. According to this study the 70 residue long domain extends on more than 40 Å in the solvent when tRNA is absent and contributes to the binding of this ligand in the complex.

For sake of clarity, the packing model in Fig. 3 highlights one AspRS-70 subunit in yellow and displays in orange the extension present in the native enzyme; this extension is about 45 amino acid long and is predicted to encompass two helices. Modeling shows that the shorter extension of the proteolyzed enzyme can be accommodated in the available solvent channels, but at the cost of some structural adaptations of the extension which likely will disturb packing. The entire extension may also be accommodated, but requires more important structural adaptation and results in a greater perturbation of contact B. This agrees with the fact that crystals of the native full length AspRS could never be obtained.

4. Concluding remarks and perspectives

In conclusion, this work exemplifies the importance of structural homogeneity for the successful crystallization of a protein. Further it shows the usefulness of protein engineering for designing proteins deprived of flexible appendices or sequence heterogeneities that can hamper crystallization by perturbing packing contacts.

From the point of view of crystallogensis, the tetragonal crystals form of yeast AspRS is a nice system to investigate poisoning of macromolecular

crystals by structural homologues. AspRS molecules of different length are already available [36] and will be used as competitor in AspRS-70 crystallization assays. These experiments should give information about the maximal length that can be incorporated without perturbing the crystal packing. The AspRS-70 tetragonal crystal form also provides an ideal model system to perform mutagenesis studies on surface residues involved in intermolecular contacts (listed in Table 3) to explore their importance in crystal packing. More important, these AspRS deletants and mutants may allow to find correlations between the nature and the surface of packing contacts and the diffraction quality of the crystals.

Acknowledgements

We wish to thank M. Frugier and P. Dumas for fruitful discussions and J. Cavarelli and D. Moras for their collaboration during structure resolution. We are also grateful to the staff of ESRF and LURE for facilities in synchrotron data collection. This work was supported by the Centre National de la Recherche Scientifique (CNRS), the European Commission (BIO4-CT98-0086 and BIO4-CT98-0189), the Centre National d'Etudes Spatiales (CNES), the Ministère de l'Éducation Nationale, de la Recherche et de la Technologie (MENRT), and Université Louis Pasteur, Strasbourg. C.S. benefited from an EC fellowship.

References

- [1] A.-C. Dock, B. Lorber, D. Moras, G. Pixa, J.-C. Thierry, R. Giegé, *Biochimie* 66 (1984) 179.
- [2] A.-C. Dock-Bregeon, D. Moras, R. Giegé, in: A. Ducruix, R. Giegé (Eds.), *Crystallization of Nucleic Acids and Proteins a Practical Approach*, 2nd edition, Oxford University Press, Oxford, 1999, p. 209.
- [3] M. Hampel, P.G. Labanauskas, L. Connors, U.L. Kirkegard, U.L. RajBhandary, P.B. Sigler, R.M. Bock, *Science* 162 (1968) 1384.
- [4] C.W. Carter, C.W. Carter Jr., *J. Biol. Chem.* 254 (1979) 12219.
- [5] R. Giegé, A.-C. Dock, D. Kern, B. Lorber, J.-C. Thierry, D. Moras, *J. Crystal Growth* 76 (1986) 554.
- [6] V. Mikol, P. Vincendon, G. Eriani, E. Hirsch, R. Giegé, *J. Crystal Growth* 110 (1991) 195.
- [7] F. Thibault, J. Langowski, R. Leberman, *J. Mol. Biol.* 225 (1992) 185.
- [8] J.D. Ng, Y.G. Kuznetsov, A.J. Malkin, G. Keith, R. Giegé, A. McPherson, *Nucleic Acids Res.* 25 (1997) 2582.
- [9] C. Sauter, B. Lorber, D. Kern, J. Cavarelli, D. Moras, R. Giegé, *Acta Crystallogr. D* 55 (1999) 149.
- [10] R. Giegé, B. Lorber, J.-P. Ebel, D. Moras, J.-C. Thierry, *C. R. Acad. Sci. Paris D-2* 291 (1980) 393.
- [11] B. Lorber, R. Giegé, J.-P. Ebel, C. Berthet, J.-C. Thierry, D. Moras, *J. Biol. Chem.* 258 (1983) 8429.
- [12] D. Moras, A.-C. Dock, P. Dumas, E. Westhof, P. Romby, J.-P. Ebel, R. Giegé, *J. Biomol. Struct. Dyn.* 3 (1985) 479.
- [13] D. Moras, A.-C. Dock, P. Dumas, E. Westhof, P. Romby, J.-P. Ebel, R. Giegé, *Proc. Natl. Acad. Sci. USA* 83 (1986) 932.
- [14] D. Moras, M. Bergdoll, *J. Crystal Growth* 90 (1988) 283.
- [15] C. Sauter, B. Lorber, J. Cavarelli, D. Moras, R. Giegé, *J. Mol. Biol.* 299 (2000) 1313.
- [16] M. Sellami, G. Prevost, J. Bonnet, G. Dirheimer, J. Gangloff, *Gene* 40 (1985) 349.
- [17] B. Lorber, D. Kern, A. Dietrich, J. Gangloff, J.-P. Ebel, R. Giegé, *Biochem. Biophys. Res. Comm.* 117 (1983) 259.
- [18] B.W. Matthews, *Methods Enzymol.* 114 (1985) 176.
- [19] Collaborative Computational Project, *Acta Crystallogr. D* 50 (1994) 760.
- [20] B. Lee, F.M. Richards, *J. Mol. Biol.* 55 (1971) 379.
- [21] S. Evans, *J. Mol. Graphics* 11 (1993) 134.
- [22] G. Kleywegt, A. Jones, *Methods Enzymol.* 277 (1997) 208.
- [23] R. Giegé, D. Moras, J.-C. Thierry, *J. Mol. Biol.* 115 (1977) 91.
- [24] D. Moras, M.-B. Comarmond, J. Fischer, R. Weiss, J.-C. Thierry, J.-P. Ebel, R. Giegé, *Nature* 288 (1980) 669.
- [25] A. Dietrich, R. Giegé, M.-B. Comarmond, J.-C. Thierry, D. Moras, *J. Mol. Biol.* 138 (1980) 129.
- [26] D. Moras, B. Lorber, P. Romby, J.-P. Ebel, R. Giegé, A. Lewitt-Bentley, M. Roth, *J. Biomol. Struct. Dyn.* 1 (1983) 209.
- [27] M. Ruff, J. Cavarelli, V. Mikol, B. Lorber, A. Mitschler, R. Giegé, J.-C. Thierry, D. Moras, *J. Mol. Biol.* 201 (1988) 235.
- [28] M. Ruff, S. Krishnaswamy, M. Boeglin, A. Poterszman, A. Mitschler, A. Podjarny, B. Rees, J.C. Thierry, D. Moras, *Science* 252 (1991) 1682.
- [29] B. Lorber, D. Kern, H. Mejdoub, Y. Boulanger, J. Reinbolt, R. Giegé, *Eur. J. Biochem.* 165 (1987) 409.
- [30] B. Lorber, H. Mejdoub, J. Reinbolt, Y. Boulanger, R. Giegé, *Eur. J. Biochem.* 174 (1988) 155.
- [31] G. Eriani, G. Prevost, D. Kern, P. Vincendon, G. Dirheimer, J. Gangloff, *Eur. J. Biochem.* 200 (1991) 337.
- [32] J. Cavarelli, B. Rees, M. Ruff, J.-C. Thierry, D. Moras, *Nature* 362 (1993) 181–184.
- [33] C. Briand, A. Poterszman, A. Mitschler, M. Yusupov, J.-C. Thierry, D. Moras, *Acta Crystallogr. D* 54 (1998) 1382.

- [34] C. Charron, C. Sauter, D.W. Zhu, J.N. Ng, D. Kern, B. Lorber, R. Giegé, *J. Crystal Growth*, in revision.
- [35] J. Janin, *Nature Struct. Biol.* 4 (1997) 973.
- [36] M. Frugier, L. Moulinier, R. Giegé, *EMBO J.* 19 (2000) 2371.
- [37] F. Agou, Y. Yang, J.-C. Gesquière, J.-P. Waller, E. Guittet, *Biochemistry* 34 (1995) 569.
- [38] J. Gangloff, G. Dirheimer, *Biochim. Biophys. Acta* 294 (1973) 263.
- [39] B. Lorber, R. Giegé, *FEBS Lett.* 156 (1983) 209.
- [40] P. Vincendon, Ph.D. Thesis, Université Louis Pasteur, Strasbourg, 1990.